Anomalous subsidiary absorption in single-crystal YIG and evaluation of spin-wave linewidth

Carl E. Patton[a] and Wolfgang Jantz[b]
Institut für Angewandte Festkörperphysik der FhG, Eckerstrasse 4, D-7800 Freiburg i. Br., West Germany

(Received 12 March 1979; accepted for publication 13 June 1979)

Measurements of the subsidiary absorption spin-wave instability threshold h_{crit} in high-quality single crystals of yttrium iron garnet reveal anomalous structure over a field interval extending several hundred Oe below the butterfly curve minimum at H_c. Such measurements have now been extended to cover the entire butterfly curve for sphere and plate samples. At the low-field end of the structure region, h_{crit} increases rapidly as the static field H is decreased to a "kink" field H'_c. As H is reduced further, the increase in h_{crit} is much more gradual. The nature of the onset changes drastically at H'_c, from a gradual increase to an abrupt jump in reflected power at threshold. Theoretical analysis of the data shows: (1) The instability at H_c is for spin waves with a polar angle θ_k of 22° rather than the 35° value often cited. (2) The field interval for the instability of zero wave number ($k = 0$) modes is not confined to $H > H_c$, but extends over a wide range down to H'_c. (3) The kink at H'_c corresponds to an abrupt transition to $k \neq 0$ spin waves at lower fields. These features are all due to the effect of the **k** dependence of ΔH_k, the spin-wave linewidth, on h_{crit}. However, a steplike increase of ΔH_k for $k \neq 0$ modes, rather than the linear dependence inferred from parallel pumping, is needed for a quantitative fit. This observation, while in partial agreement with the existing three-magnon confluence theory, shows the need for a refined calculation. The structure between H_c and H'_c varies with sample shape and appears to be related to low-k magnetostatic mode excitations in the spin-wave spectrum.

PACS numbers: 75.30.Ds, 75.50.Gg, 76.50. + g

I. INTRODUCTION

The parametric excitation of spin waves at high microwave power levels has been of interest since the discovery of subsidiary absorption and the subsequent explanation by Suhl[1]. The conventional interpretation of subsidiary absorption involves the excitation of spin waves with nonzero wavenumber k propagating at an angle $\theta_k \simeq 35°$ with respect to the static field H, for H below the butterfly curve minimum at H_c. In this field range, the threshold microwave field h_{crit} and wave number k are generally taken to increase with decreasing field. In the field interval above H_c up to the cutoff field for first-order spin-wave instability, k is near zero and θ_k decreases.[2]

Recent high-power data on single-crystal YIG reveal a number of peculiar effects which are inconsistent with the above interpretation: (1) Butterfly curves[3] showed a broad flat minimum which extended to several hundred Oe below the butterfly curve minimum at H_c, rather than the smooth increase predicted theoretically. (2) Data obtained with a new cw technique showed a pronounced structure in the instability onset superimposed on the broad minimum noted above.[4,5]

Additional data have now been obtained on oriented plates and spheres of high-quality single-crystal YIG. The analysis of these data by a recent theory[6] which includes crystalline anisotropy and the **k** dependence of the spin-wave linewidth ΔH_k indicates that significant revisions in the old interpretations of subsidiary absorption in narrow linewidth single-crystal ferrites are needed. The key result involves the **k** dependence of ΔH_k. Appropriate dependences allow the various prominent peculiarities of the measured threshold curves to be interpreted very satisfactorily. As a result, a better understanding of instability processes is obtained as well as important results concerning the functional dependence of ΔH_k on wave vector **k**.

II. EXPERIMENTAL RESULTS

Subsidiary absorption data were obtained on single-crystal YIG spheres and thin plates at room temperature and 9.16 GHz with a modified Varian 4500 EPR spectrom-

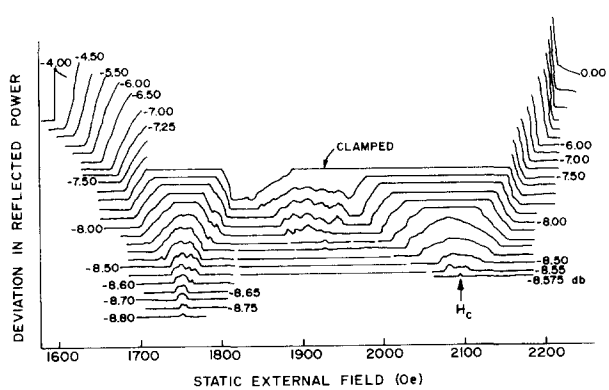

FIG. 1. Typical recorder traces demonstrating the acquisition of instability data. The reflected power is monitored as a function of static field as the latter is swept slowly while the incident power level, denoted in dB below the maximum power, is held constant. Points at which the recorder traces first deviate from a given baseline indicate threshold values.

[a]Address: Department of Physics, Colorado State University, Fort Collins, Colorado 80523.
[b]Presently Visiting Scientist at IBM, Thomas J. Watson Research Center, Yorktown Heights, NY 10598.

 0021-8979/79/117082-07$01.10 © 1979 American Institute of Physics

Downloaded 09 May 2003 to 129.82.31.230. Redistribution subject to AIP license or copyright, see http://ojps.aip.org/japo/japcr.jsp

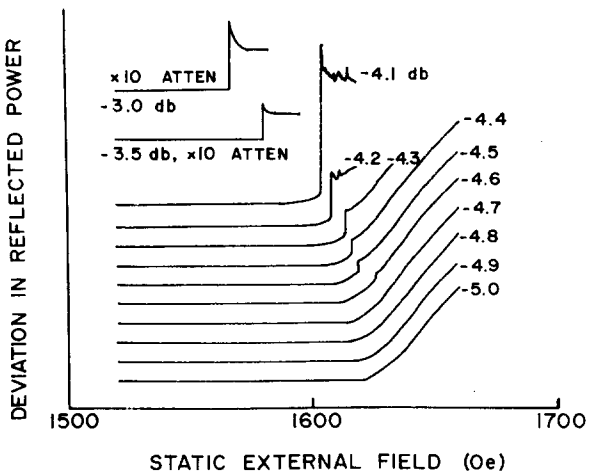

FIG. 2. Recorder traces similar to those in Fig. 1 but on an expanded field scale, to demonstrate the change in the character of the instability onset.

eter. Butterfly curves of the instability threshold h_{crit} as a function of H were obtained by sweeping the static field with the microwave field held constant and noting the instability threshold point as discussed in Ref. 5. Data were obtained at higher power levels than normally possible with such spectrometers at room temperature by using the Varian Dewar insert in the cavity. This resulted in a dielectric microwave field concentration at the sample position and allowed measurement of h_{crit} over the entire field range for subsidiary absorption. The power enhancement at the sample due to the Dewar insert was about 3.5– 4.0 dB.

Some typical onset data are shown in Fig. 1 for a [111] magnetized YIG sphere with the microwave field along [1$\bar{1}$0]. The procedure was to sweep the static field (horizontal axis) while monitoring the change in reflected power from the cavity (vertical deviations from each baseline). The incident power levels in dB, relative to the maximum power available, are indicated for each trace. One sees the first increases in reflected power at $H = 2100$ Oe and an incident power of -8.55 dB. This corresponds to the usual butterfly curve minimum, denoted by H_c and h_{crit}^{min}.

As the power is increased, the two threshold points separate in field. The high-field points approach a maximum about 2200 Oe at very high powers. This coresponds to the cutoff for first-order instability as the bottom edge of the spin-wave manifold moves above the frequency of the pumped magnons at half the excitation frequency, 4.58 GHz. The theoretical cutoff for [111] magnetized YIG occurs at 2161 Oe. The apparent cutoff of 2212 Oe in Fig. 1 is higher by 2.3%, presumably due to Hall effect gaussmeter calibration error. To compensate for this small mismatch and to facilitate detailed comparison of butterfly curve data with theory, the experimental field values were adjusted downward by the above factor for the results shown in Figs. 2 and 4 – 12. The low-field points move down in fields as the power is increased. Additional local minima appear in the instability curve near 1900 and 1750 Oe. This three-minima structure in the butterfly curve for single-crystal YIG was reported previously.[4,5]

The onset behavior for fields below 1600 Oe and powers above about -4.5 dB are of particular interest. Note the curve for -4.5 dB in Fig. 1, for example. The initial onset appears to be similar to those at lower powers, but a small abrupt jump occurs about 20 Oe above the threshold position. Further increases in the incident power cause this abrupt change in reflected power to move closer to the threshold point. This behavior is shown systematically in Fig. 2. The small jump first becomes apparent at about -4.6 dB. As the power increases, the size of the jump increases and it moves closer in field to the threshold point. At powers in excess of about -3.5 dB, the jump actually defines the threshold. At these higher powers, peculiar hysteresis effects are also observed. It is evident from these observations that the distinct change in the character of the instability onset is brought about by two competing processes. At powers below about -4.0 dB, the process giving the gradual onset is preferred. At higher powers, the process giving the jumplike onset dominates.

Data similar to that in Figs. 1 and 3 were used to construct conventional butterfly curves of h_{crit} versus H. The power enhancement provided by the Dewar insert made it possible to obtain data down to a static field of 800 Oe for spherical samples. Typical results for a [111] magnetized sphere are given in Fig. 3. The calibration from incident power in dB below maximum power to microwave field amplitude was based on an assumed threshold field $h_{crit}^{min} = 0.5$ Oe for the butterfly curve minimum at $H = H_c$. No absolute calibration was attempted because of the field distortions of the cavity insert, but the above values are typical of high-quality single-crystal YIG at room temperature. Absolute calibration is not critical for the present purposes, as will be evident from the discussions to follow.

The butterfly curve in Fig. 3 exhibits several features which suggest modifications in the generally accepted interpretations of instability processes for ferrites. Of particular importance are: (1) The distinct kink at $H_c' = 1525$ Oe, (2) the very gradual decrease in h_{crit} for fields below H_c', (3) the initial rapid decrease in h_{crit} for fields just above H_c', (4) the relatively flat region from 1700 to 2050 Oe and the distinct

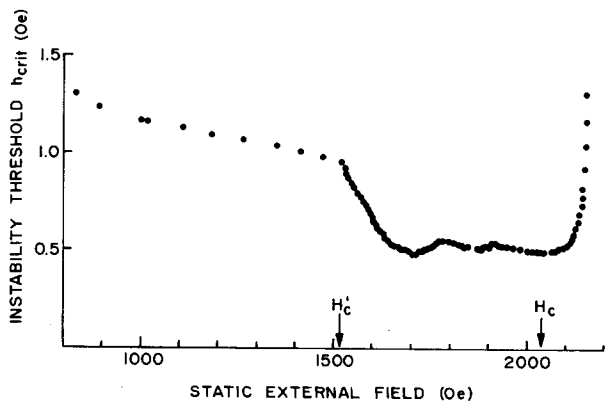

FIG. 3. A typical butterfly curve of threshold microwave amplitude h_{crit} versus static field for the [111] magnetized sphere, with the microwave pump field at 9.16 GHz parallel to [1$\bar{1}$0]. The curve was constructed from data similar to that in Fig. 1, assuming a minimum threshold, $h_{crit}^{min} = 0.5$ Oe, at H_c for calibration purposes.

Downloaded 09 May 2003 to 129.82.31.230. Redistribution subject to AIP license or copyright, see http://ojps.aip.org/japo/japcr.jsp

structure in this region, and (5) the shift of the conventional butterfly curve minimum from the position observed in polycrystals (1800–1900 Oe) to the higher value of 2050 Oe. In subsequent sections it will be shown that all these features can be explained by suitable refinements of the theory. The only quantitative feature of the data in Fig. 3 which is already consistent with the previous interpretations is the rapid increase in h_{crit} as the field approaches the value corresponding to the crossing of the lower edge of the spin-wave manifold above one-half the pump frequency ω. First-order processes are not allowed above this field and the threshold diverges.

III. ANALYSIS AND DISCUSSION

Butterfly curve data as shown in Fig. 2 have been analyzed using a generalized instability theory for linear transverse pumping which includes the influence of crystalline anisotropy and the **k** dependence of the spin-wave linewidth ΔH_k on the threshold.[6] It is found that the **k** dependence of ΔH_k has a very strong effect on the detailed shape of the butterfly curve. A systematic examination of various functional dependences for $\Delta H_k(\mathbf{k})$ and the resulting theoretical butterfly curves has been made. Comparison of these results with the present data leads to a number of important revisions in the conventional interpretation of subsidiary absorption.

A. Angle of the unstable spin waves

The first such revision concerns the generally accepted result that transverse pumping promotes the instability of spin waves with **k** at about 35° to the static field. When the spin-wave linewidth is large, this is generally true. The result is a butterfly curve minimum at $H_c \simeq 1900$ Oe related to spin waves with wavenumber $k \to 0$ propagating at $\theta_k \simeq 35°$. For reasons to become clear later, this behavior relies on a large contribution to ΔH_k which does not depend on θ_k. Such contributions do occur in polycrystalline ferrites and in single crystals containing relaxing impurities. For low-loss single crystals, however, the θ_k dependence of ΔH_k contributes significantly to the overall linewidth and tends to decrease the "preferred" θ_k value for the modes with the lowest threshold. This, in turn, pushes the butterfly curve minimum to higher field.[7]

Figure 4 shows two theoretical curves for which ΔH_k was adjusted to give a minimum h_{crit} of 0.5 Oe, to facilitate

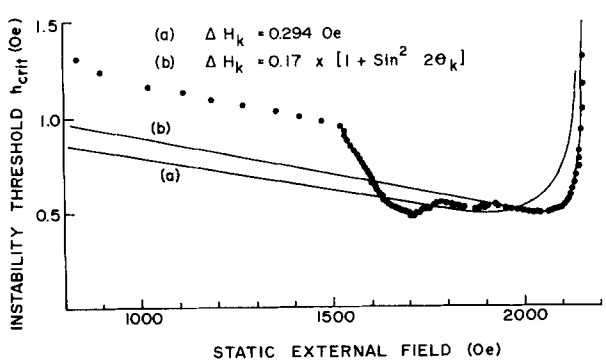

FIG. 4. Theoretical fits to the butterfly curve of Fig. 3 for two trial functions for the spin-wave linewidth as described in the text.

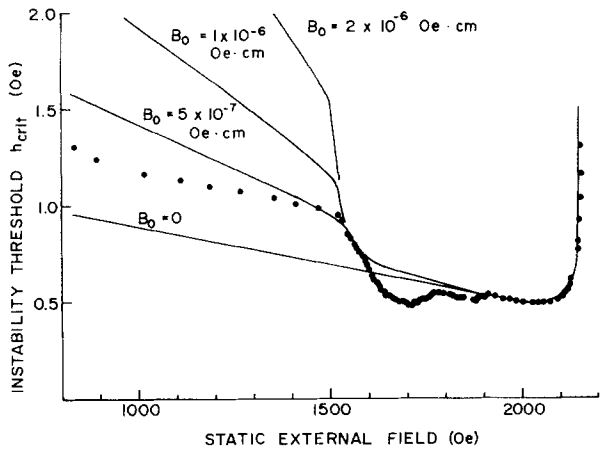

FIG. 5. Theoretical fits to the butterfly curve of Fig. 3 for a trial function which includes a linear k dependence for the spin-wave linewidth as described in the text.

comparison with the data in Fig. 3. For curve (a), ΔH_k was taken constant. As noted above, this results in a minimum at 1875 Oe, corresponding to $\theta_k \simeq 34°$. Curve (b) was calculated with a trial function,

$$\Delta H_k = A_0(1 + \sin^2 2\theta_k), \tag{1}$$

with $A_0 = 0.17$ Oe. This value of A_0 provides a rather good fit to the experimental data in the vicinity of the minimum at 2025 Oe and at higher fields. The fit is poor at low fields because, as shall be seen, no k dependence is included in Eq. (1). The minimum point for curve (b) is for $\theta_k \simeq 22°$. It is quite satisfying that the θ_k dependence in Eq. (1) was also found to provide an optimum fit to parallel pumping data in single crystals.[8]

B. Wave number of the unstable spin waves

It is well known that h_{crit} should increase more rapidly with decreasing field indicated by the curves in Fig. 4 due to the increase in ΔH_k with wave number k.[2,9] The lack of such a k dependent term in Eq. (1) results in theoretical curves which fall well below the data. Magnon confluence processes make a significant contribution to this k dependence.[9] In the k range accessible for subsidiary absorption, with k generally below 10^6 cm^{-1}, the dependence is usually assumed to be linear. Figure 5 shows the results of calculations for a trial ΔH_k function of the form

$$\Delta H_k = A_0(1 + \sin^2 2\theta_k) + B_0 k, \tag{2}$$

with $A_0 = 0.17$ Oe as before, and various values of B_0 as indicated on the plot.

These fits provide several remarkable clues to the new results of this investigation. It is seen that the k dependence of ΔH_k results in a steep increase in h_{crit} with decreasing field in the vicinity of 1500 Oe which qualitatively reproduces the experimental kink effect. Consequently, the calculations can be used to clarify how the kink is produced. The results follow: As H_c' is approached from the low-field side, the theoretical k values corresponding to the threshold are relatively large, on the order of 10^5 cm^{-1}. As H increases above H_c', the theory indicates an abrupt jump to $k \simeq 0$. The

Downloaded 09 May 2003 to 129.82.31.230. Redistribution subject to AIP license or copyright, see http://ojps.aip.org/japo/japcr.jsp

kink field, therefore, represents a transition point from high-k unstable modes to low-k unstable modes. This is remarkably consistent with the results in Figs. 1 and 2, which demonstrate a drastic change in character of the instability onset at H_c'. This kink effect will be considered more explicitly shortly.

Finally, it is clear that a linear k term in ΔH_k is not adequate to provide a quantitative fit to the data below 1500 Oe. The data points at low field define a line which is roughly parallel to the theoretical curve for $B_0 = 0$ (no k dependence in ΔH_k), but is shifted up by about 0.3 Oe. This comparison suggests that the k dependence of ΔH_k is more like a step function than a linear function of k.

The theory for three-magnon confluence relaxation does, in fact, indicate that the k dependence of ΔH_k should be linear in k only for k below some cutoff value on the order of 10^5–10^6 cm^{-1}. The theory[9] suggests a linewidth k-dependent term of the form $B_1 L(k/k_c)$, with the L function defined as

$$L(x) = \frac{1}{1.39x} \ln\left(1 + \frac{8x^2(1+2x^2)}{1+8x^2}\right). \tag{3}$$

This L function is plotted in Fig. 6 as a function of x. The function is reasonably linear for $x < 0.1$, peaks at $x \simeq 0.5$, and trails off rather slowly for large x. If the k_c for subsidiary absorption were sufficiently small, i.e., smaller than twice the wave number observed just below H_c', the dependence in Fig. 6 for ΔH_k versus k would constitute a reasonable approximation to the step function suggested by the data.

A series of theoretical curves have been generated with a trial function,

$$\Delta H_k = A_0(1 + 2\sin^2 2\theta_k) + B_1 L\left(\frac{k}{k_c}\right), \tag{4}$$

for various values of k_c and B_1 adjusted to fit the experimental data at $H = 1350$ Oe. By forcing a fit at one intermediate low-field point, it is possible to see if any reasonable k_c value can simultaneously match both the slope of the data below H_c' and the behavior near the kink. Representative curves are shown in Fig. 7 for four k_c values. It appears that the best fit occurs for some value between 10^4 and 10^6 cm^{-1}. The trial function yields good fits to the low-field behavior and the

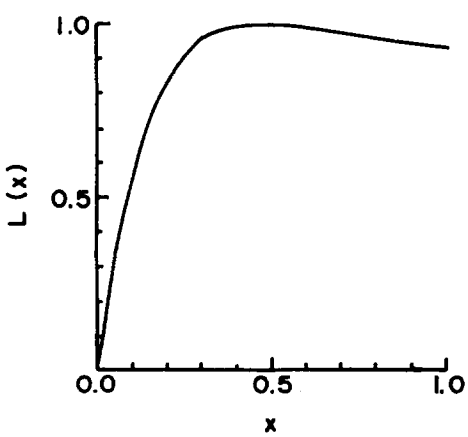

FIG. 6. The function $L(x)$ in the three-magnon confluence relxation theory of Sparks *et al.* (Ref. 9).

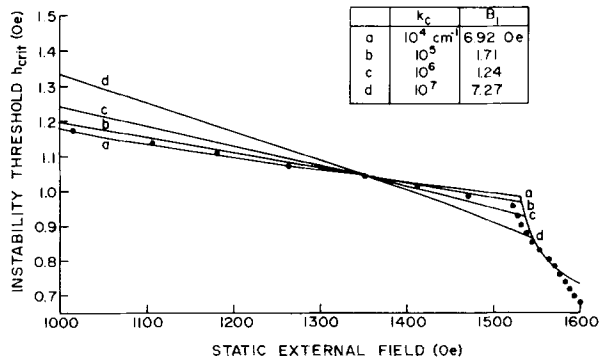

FIG. 7. Theoretical fits to the butterfly curve of Fig. 3 in the vicinity of the kink field H_c' for a trial function based on the general three-magnon confluence relaxation dependence on wave number k, as discussed in the text.

kink effect. Recall that the low field, relatively flat region corresponds to the instability of high-k ($\sim 10^5$ cm^{-1}) spin waves. Above H_c', the modes have much lower k values which are essentially zero within the framework of the theory.

The parameters $B_1 = 1.71$ Oe and $k_c = 10^5$ cm^{-1}, which yield the "best fit" in Fig. 7, may be compared with the theoretical values in the confluence theory. Utilizing various approximations in the theory, Sparks[9] obtains a value $B_1 \simeq 0.16$ Oe and $k_c \simeq 8.5 \times 10^5$ cm^{-1}. Thus, it appears that the functional form of the spin-wave linewidth from the confluence theory is reasonably correct, but that the quantitative expressions for the parameters in the theory are not quite right. A further problem is that the theory in its published form does not predict any θ_k dependence except in the limit of low-k values. The postulation is definitely inconsistent with the present results. In view of the excellent fit obtained in Fig. 7, it appears that a more rigorous calculation of three-magnon confluence relaxation is in order.

The values of B_1 and k_c which provide a reasonable fit to the present subsidiary absorption data deviate substantially from those values which provide good fits to parallel pumping data in similar single crystals.[8] From the parameters in Ref. 8, k_c can be estimated to be at least 10^6 cm^{-1} and B_1 to be smaller than 0.1 Oe. Thus, independent fits to data for subsidiary absorption and parallel pumping appear quite good when considered alone, but imply linewidth parameters which are over an order of magnitude different. The effect of these differences is most peculiar. For subsidiary absorption, the small k_c pushes the $L(x)$ function over the top for almost all of the high k values so that ΔH_k is essentially a step function in k. In parallel pumping, we have the opposite effect. Here, k_c is so large that the $L(x)$ function yields a linear k dependence for all but the highest acceessible k values. Realizing that one weak point in the theory is the lack of a rigorous prediction of the θ_k dependence of these parameters, and that θ_k is rather different for the processes, such problems merely underscore the need for a more rigorous confluence theory.

C. The kink effect and $k = 0$ modes

Figure 8 presents a comparison between the sphere data

Downloaded 09 May 2003 to 129.82.31.230. Redistribution subject to AIP license or copyright, see http://ojps.aip.org/japo/japcr.jsp

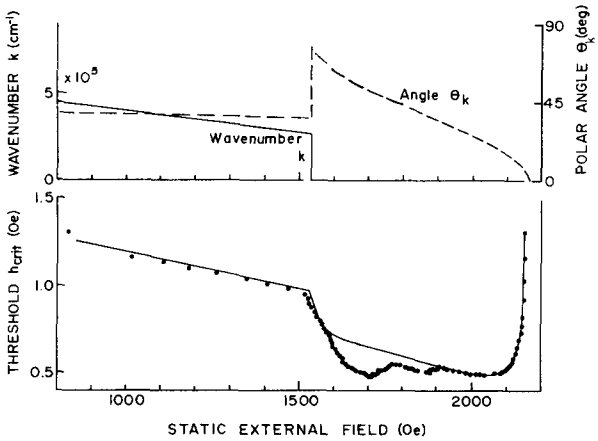

FIG. 8. Theoretical fit to the butterfly curve data of Fig. 3 corresponding to curve (b) of Fig. 7 with companion plots of the wave number k and spin-wave angle θ_k for the unstable modes.

and the full theoretical butterfly curve corresponding to curve (b) in Fig. 7, based on the trial function of Eq. (4) with $A_0 = 0.17$ Oe, $B_1 = 1.17$ Oe, and $k_c = 10^5$ cm^{-1}. Except for the low part of the flat region between 1600 and 1900 Oe, the quantitative agreement is rather remarkable. The remaining minor discrepancies will be discussed in Sec. III D.

The two upper curves in Fig. 8 show the nature of the unstable spin waves that yield the theoretical h_{crit} values described by the lower curve. As the static field increases from the lowest values, the θ_k values remain approximately constant and the wave number decreases slowly until the kink point is reached. As the field exceeds the kink value, the k value for the unstable mode drops abruptly to zero. This forces a jump in θ_k up to about 80°. As the field is further increased, k remains zero and θ_k decreases smoothly to $\theta_k = 0$ at the cutoff field for subsidiary absorption.

The kink effect and the abrupt jumps in k and θ_k at the kink field can be explained by considering the instability threshold for a general (k, θ_k) magnon state,[8] i.e.,

$$h_c = \frac{\omega}{\omega_m} \frac{\Delta H_k}{\sin\theta_k \cos\theta_k} \frac{1}{f(\theta_k)\alpha(H,\omega)}, \tag{5}$$

where ω is the pump frequency, $\omega_m = \gamma 4\pi M_0$ expresses the saturation induction $4\pi M_0$ in angular frequency units, $\alpha(H,\omega)$ designates the normalized uniform precession or ferromagnetic resonance amplitude, and $f(\theta_k)$ is given by

$$f(\theta_k) = \tfrac{1}{2}[(\omega_m^2 \sin^4\theta_k + \omega^2)^{1/2} - \omega_m^2 \sin\theta_k] + \tfrac{1}{2}\omega. \tag{6}$$

The gyromagnetic ratio γ is taken as positive. Strictly speaking, the linear polarized microwave pump field introduces a dependence of h_c in Eq. (5) on the azimuthal spin-wave angle ϕ_k.[10] The presence of crystalline anisotropy[6] also modifies the form but not the substance of Eq. (5). In the interest of clarity, both effects have been neglected in the discussion to follow. For the quantitative calculations, however, the complete theoretical formulation of Ref. 6 was used. The uniform precession amplitude in the subsidiary absorption region corresponds to fields substantially below those required for ferromagnetic resonance. In this region, $\alpha \propto (\omega - \omega_0)^{-1}$ is satisfied, with $\omega_0 = \gamma H$, so that α decreases as the field decreases. This causes the threshold to increase, as indicated by the $B_0 = 0$ curve in Fig. 5.

It is to be emphasized that h_c is not the observed threshold, but simply represents the possible thresholds as a function of θ_k for fixed H and ω. The polar angle θ_k is related to the wave number k through the dispersion relation for the spin-wave frequency ω_k, which is given by

$$\left(\frac{\omega_k}{\gamma}\right)^2 \simeq (H_i + Dk^2)(H_i + Dk^2 + 4\pi M_0 \sin^2\theta_k), \tag{7}$$

where H_i is the internal effective static field, including demagnetizing and anisotropy terms for [111] magnetized YIG, and D is the exchange parameter. The observed threshold at any given h_{crit} static field H will simply be the *minimum* h_c, when all the available spin-wave states at $\omega_k = \frac{1}{2}\omega$ are considered. Even though the minimization procedure is complicated and best done numerically (as it was for the curves presented above), the qualitative reasons for the kink effect and the (k, θ_k) dependencies in Fig. 8 can be made readily evident.

The key is in the realization that the explicit θ_k terms in Eq. (5) and the ΔH_k term promote a minimum h_c at different θ_k values. The explicit terms have a minimum at $\theta_k \simeq 35°$ for YIG at X band. The ΔH_k **k** dependence, on the other hand, makes ΔH_k minimum for k as low as possible, corresponding to $\theta_k = 90°$. Such considerations are subject, of course, to the constraints imposed by $\omega_k = \frac{1}{2}\omega$ on the available (k,θ_k) states under given bias conditions. The opposing preferences for $\theta_k \simeq 35°$ and $k \simeq 0$ indicated above lead directly to the kink effect.

In order to better visualize the trade-offs and dispersion constraints, consider the schematic dispersion diagrams in Fig. 9. The spin-wave manifold of ω_k versus k for the $0 < \Theta_k < \frac{1}{2}\pi$ is shown for two different fields. Diagram (a) is for H well below H_c' so that the available modes at $\omega_k = \frac{1}{2}\omega$ are well above the upper $\theta_k = \frac{1}{2}\pi$ branch of the manifold at $k = 0$. Under these conditions, the smallest available k value is still well above k_c. As a consequence, no significant reduction in ΔH_k can be achieved by reducing k. The explicit θ_k terms, therefore, dominate to provide a minimum h_c at θ_k

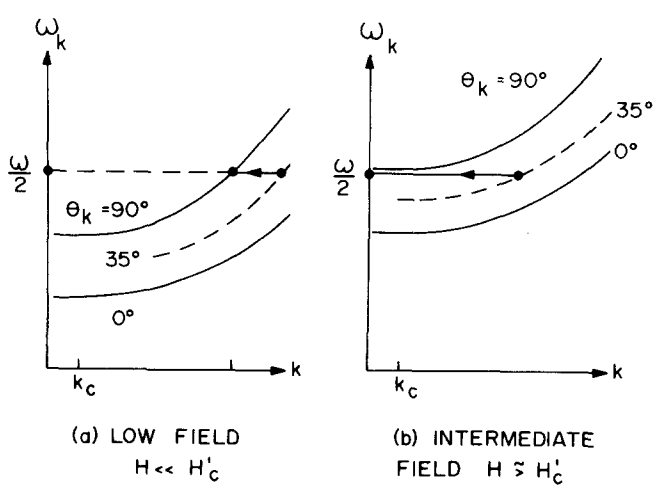

FIG. 9. Schematic illustrations of the spin-wave manifold under low-field and intermediate-field bias as discussed in the text.

Downloaded 09 May 2003 to 129.82.31.230. Redistribution subject to AIP license or copyright, see http://ojps.aip.org/japo/japcr.jsp

$\simeq$35°. This is evident from the dashed θ_k curve in Fig. 8 for fields below 1525 Oe.

Diagram (b) in Fig. 9 shows the spin-wave manifold for a somewhat higher H so that the smallest available k value is well below k_c. In practical terms, with $k_c \simeq 10^5$ cm^{-1}, this means that $k \simeq 0$ is available. In this case, it is seen that a substantial reduction in ΔH_k can be achieved by reducing k. In the event that this reduction is large enough to override the θ_k preference, the unstable mode with the lowest threshold will now be a $k \simeq 0$ and high θ_k mode. These considerations are well demonstrated by the k and θ_k curves in Fig. 8. As H increases above 1525 Oe, the availability of $k \simeq 0$ modes and the lower ΔH_k for $k = 0$ promotes an abrupt shift from high k and $\theta_k \simeq 35°$ to $k \simeq 0$ and $\theta_k \simeq 80°$. At higher fields, the $k \simeq 0$ preference is retained and the dispersion constraint allows θ_k to decrease.

To obtain the discontinuous behavior of k at H_c', it is not imperative to have a $L(x)$-type ΔH_k k dependence. It occurs for a linear k dependence as well, as shown by the theoretical curves in Fig. 5.

The instability theory elaborated by Suhl[1] strictly applies to the pumping of $k \neq 0$ spin waves only, insofar as surface dipole terms are neglected. The result of this investigation, $k = 0$ for $H > H_c'$, at first glance appears to be inconsistent with this underlying assumption. However, the computer analysis requires $k = 0$ only in the sense that the Dk^2 exchange contribution to the magnon energy and the k-dependent contribution to ΔH_k be negligible. These conditions are also met by small $k < 10^4$ cm^{-1}. In fact, the observation and analysis of standing spin-wave spectra around the butterfly curve minimum at 2050 Oe gives direct evidence that such low-k spin waves are actually excited at threshold.[4,5]

The explanation of the kink at H_c' in terms of two different competing instabilities, with $k \neq 0$ instability below H_c' and $k \simeq 0$ instability above H_c' correlates nicely with the abrupt change in the character of the onset shown in Fig. 2.

D. Magnetostatic mode instability

The only remaining problem concerns the complicated structure over the flat region of the butterfly curve from about 1600 to 1900 Oe. In Fig. 3, one very prominent dip is evident at 1700 Oe and a second shallow dip is seen at about 1870 Oe. More detailed measurements over this field region are summarized in Fig. 10. The results show that, in addition to these two major dips, there are a number of other small dips and shoulders. Assuming that this field region does correspond to the instability of low-k modes as the preceeding analysis suggests, it is apparent from Figs. 8 and 10 that a simple continuum picture for low-k spin waves is not valid, and that low-k modes which are driven unstable have lower thresholds than predicted from the continuum theory.

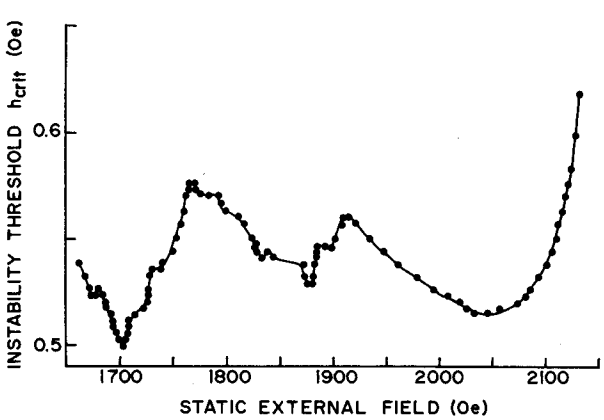

FIG. 10. Detailed data of h_{crit} versus static field over the $k \simeq 0$ region of the butterfly curve above the kink field H_c'.

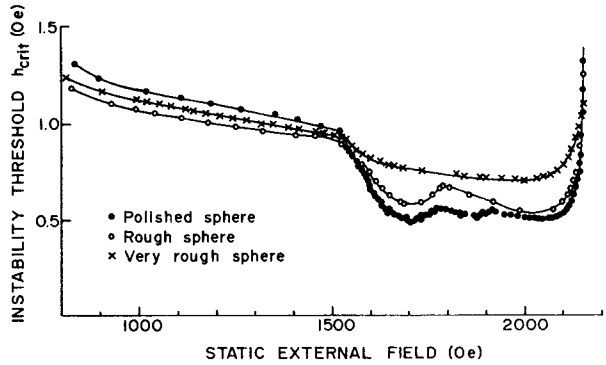

FIG. 11. Butterfly curve data for YIG spheres with varying degrees of surface roughness.

In view of these conclusions, one natural interpretation of the structure in Fig. 8 is in terms of magnetostatic modes. The magnetostatic mode spectrum for spheres has three prominent peaks.[11] Expressed in terms of the θ_k values at $k = 0$, these modes lie at approximately 39°, 54°, and 63° for the [210], [110], and [220] modes, respectively. Close inspection of Fig. 8 shows that the first two θ_k values correspond very closely to the dips at 1870 and 1700 Oe. These identifications provide rather convincing arguments that the complicated structure under discussion here is related to magnetostatic modes. The structure is also independent of crystallographic orientation and is not related to anisotropy considerations.

In contrast, qualitatively similar dips observed for parallel pumping butterfly curves[8] rely decisively on the anisotropy of both the parametric coupling and the spin-wave dispersion and, therefore, depend on the orientations of both **H** and **k** relative to the cubic axes. This is not the case here.

Two further tests of the magnetostatic mode hypothesis were carried out. In the first test, butterfly curve data were obtained on a series of YIG spheres with varying degrees of surface roughness. The idea was to exploit the fact that surface imperfections selectively increase the damping of magnetostatic modes, whereas high-k spin-wave modes are rather insensitive to the surface condition. Roughening the surface, therefore, should reduce the influence of magnetostatic modes and result in better agreement with the theory which neglects surface dipole terms altogether. These measurements are shown in Fig. 11. The data are consistent with the above expectations; the structure in the high-field flat region tends to wash out, along with a general increase in h_{crit}, whereas the h_{crit} points below the kink field are hardly affected.

In the second test, data were obtained in in-plane and

Downloaded 09 May 2003 to 129.82.31.230. Redistribution subject to AIP license or copyright, see http://ojps.aip.org/japo/japcr.jsp

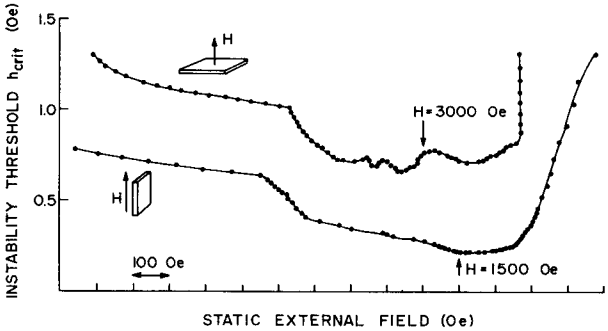

FIG. 12. Butterfly curve data for in-plane and normally magnetized YIG plates.

normally magnetized YIG plates. It is well known that the magnetostatic mode spectrum is quite different for these two configurations than for spheres.[12] One would expect that the differences would show up in the butterfly curves. The results are given in Fig. 12. The horizontal field axes are different for the two configurations, mainly due to the different demagnetizing fields. It is evident that the kink effect occurs for both orientations, but that the shapes of the butterfly curves above H_c' are quite different. Considerable structure is evident for the normally magnetized plate, as well as a very abrupt increase in h_{crit} right at the cutoff field for subsidiary absorption. These characteristics are consistent with the predominance of resolvable magnetostatic modes near the bottom edge of the spin-wave manifold for the perpendicular configuration. Very little structure is seen for the in-plane magnetized plate. For this configuration, the resolvable mangetostatic modes occur at the top of the manifold, which corresponds to fields below H_c'. These modes cannot affect the butterfly curve because, in this field range, high-k spin waves determine the threshold.

IV. SUMMARY AND CONCLUSION

The above discussion has presented experimental data on subsidiary absorption instability and the related butterfly curves for such processes for high-quality YIG single crystals. These results have been considered within the framework of a refined spin-wave instability theory, with the wave-vector dependence of the spin-wave linewidth taken explicitly into account. It is found that the butterfly curves, as well as the character of the instability onset, differ significantly from those which have commonly been assumed for single crystals. Almost all of the observed differences can be attributed to some aspect of the spin-wave linewidth **k** dependence.

The first such effect is a shift of the butterfly curve minimum by several hundred Oe due to the θ_k dependence of ΔH_k. This results in a minimum at $\theta_k \simeq 22°$, a value which is much lower than usually assumed. Empirically, the constant term in ΔH_k and the coefficient multiplying the $\sin^2 2\theta_k$ angle term turn out to be approximately equal for the samples investigated here.

The second result concerns the k dependence of ΔH_k and its effect on the shape of the butterfly curve. The gradual increase in h_{crit} with decreasing field at low field implies that the critical wave number k_c in the k-dependent magnon confluence ΔH_k term is very small, on the order of 10^5 cm^{-1}. The effect of this small k_c is to make ΔH_k essentially a step function of k, with a nearly constant contribution to ΔH_k for $k \neq 0$ compared with the value for $k \simeq 0$ modes.

This k-dependent term in ΔH_k also results in a kink in the butterfly curve at a critical static field H_c' at which an abrupt transiton from the instability of high-k modes to the instability of low-k modes occurs. This effect manifests itself both in the shape of the butterfly curve and in a change in the character of the instability onset.

The final effect is a result of the magnetostatic mode interactions at fields above H_c'. Depending on the sample shape and surface polish, considerable structure in the butterfly curve may or may not occur in the field region where the instability of $k \simeq 0$ modes is preferred. When this structure exists, the corresponding h_{crit} values are generally below the theoretical values for $k \simeq 0$ spin waves. The structure, moreover, to a certain extent duplicates the magnetostatic mode spectrum. Thus, it appears that at least over part of this wide $k \simeq 0$ instability region, the magnetostatic modes play an important role in giving the butterfly curve considerable structure by reducing the threshold below the values expected from the continuum theory.

ACKNOWLEDGMENTS

This work was supported in part by the Alexander von Humboldt Foundation and the U.S. Army Research Office, Grant No. DAAG 29-77-G-0209. The YIG samples have been kindly supplied by W. Tolksdorf, Philips Research Laboratories, Hamburg, Germany.

[1]H. Suhl, J. Phys. Chem. Solids **1**, 209 (1957).
[2]C.E. Patton, in *Magnetic Oxides*, edited by D.J. Craik (Wiley, London, 1975), pp. 575–645.
[3]Y.M. Yakovlev, N.Y. Burdin, Y.R. Shilnokov, and T.N. Bushueva, Sov. Phys. Solid State **12**, 2475 (1971).
[4]W. Jantz, dissertation, Universität Freiburg, 1974.
[5]W. Jantz and J. Schneider, Phys. Status Solidi A **31**, 595 (1975).
[6]C.E. Patton, Phys. Status Solidi (to be published).
[7]C.E. Patton, J. Appl. Phys. **41**, 431 (1970).
[8]C.E. Patton and W. Jantz, IEEE Trans. Magn. MAG-**14**, 698 (1978).
[9]See E. Schlömann, Phys. Rev. **121**, 1312 (1961); M. Sparks, R. Loudon, and C. Kittel, Phys. Rev. **122**, 791 (1961); M. Sparks, *Ferromagnetic Relaxation Theory* (McGraw-Hill, New York, 1964), pp. 95–100.
[10]C.E. Patton, J. Appl. Phys. **40**, 2837 (1969).
[11]See, for example, P. Röschmann, IEEE Trans. Magn. MAG-**11**, 1247 (1975).
[12]R.W. Damon and J. R. Eshbach, J. Phys. Chem. Solids **19**, 308 (1961).

Downloaded 09 May 2003 to 129.82.31.230. Redistribution subject to AIP license or copyright, see http://ojps.aip.org/japo/japcr.jsp